NIH-PA Author Manuscript

NIH-PA Author Manuscript

NIH-PA Author Manuscript

SPFH1 and SPFH2 Mediate the Ubiquitination and Degradation of Inositol 1,4,5-Trisphosphate Receptors in Muscarinic Receptor-Expressing Hela Cells

Yuan Wang,
Department of Pharmacology, SUNY Upstate Medical University, 750 E. Adams Street, Syracuse, NY 13210, USA

Margaret M.P. Pearce,
Department of Pharmacology, SUNY Upstate Medical University, 750 E. Adams Street, Syracuse, NY 13210, USA

Danielle A. Sliter,
Department of Pharmacology, SUNY Upstate Medical University, 750 E. Adams Street, Syracuse, NY 13210, USA

James A. Olzmann,
Department of Biology, Stanford University, Palo Alto, CA 94305, USA

John C. Christianson,
Department of Biology, Stanford University, Palo Alto, CA 94305, USA

Ron R. Kopito,
Department of Biology, Stanford University, Palo Alto, CA 94305, USA

Stephanie Boeckmann,
Department of Pharmacology, SUNY Upstate Medical University, 750 E. Adams Street, Syracuse, NY 13210, USA

Christine Gagen,
Department of Pharmacology, SUNY Upstate Medical University, 750 E. Adams Street, Syracuse, NY 13210, USA

Gil S. Leichner,
Bert W. Strassburger Lipid Center, Sheba Medical Center, Tel Hashomer, 52621 ISRAEL

Joseph Roitelman, and
Bert W. Strassburger Lipid Center, Sheba Medical Center, Tel Hashomer, 52621 ISRAEL

Richard J.H. Wojcikiewicz
Department of Pharmacology, SUNY Upstate Medical University, 750 E. Adams Street, Syracuse, NY 13210, USA

Summary

Address correspondence to: R.J.H. Wojcikiewicz, Department of Pharmacology, SUNY Upstate Medical University, 750 East Adams Street, Syracuse, NY 13210. Tel: (315) 464 7956; Fax: (315) 464 8014; wojcikir@upstate.edu.

Inositol 1,4,5-trisphosphate (IP$_3$) receptors are endoplasmic reticulum (ER) membrane calcium channels that, upon activation, become substrates for the ER-associated degradation (ERAD) pathway. While it is clear that IP$_3$ receptors are polyubiquitinated and are transferred to the proteasome by a p97-based complex, currently very little is known about the proteins that initially select activated IP$_3$ receptors for ERAD. Here, we have transfected HeLa cells to stably express m3 muscarinic receptors to allow for the study of IP$_3$ receptor ERAD in this cell type, and show that IP$_3$ receptors are polyubiquitinated and then degraded by the proteasome in response to carbachol, a muscarinic agonist. In seeking to identify proteins that mediate IP$_3$ receptor ERAD we found that both SPFH1 and SPFH2 (also known as erlin 1 and erlin 2), which exist as a hetero-oligomeric complex, rapidly associate with IP$_3$ receptors in a manner that precedes polyubiquitination and the association of p97. Suppression of SPFH1 and SPFH2 expression by RNA interference markedly inhibited carbachol-induced IP$_3$ receptor polyubiquitination and degradation, but did not affect carbachol-induced calcium mobilization or IκBα processing, indicating that the SPFH1/2 complex is a key player in IP$_3$ receptor ERAD, acting at a step after IP$_3$ receptor activation, but prior to IP$_3$ receptor polyubiquitination. Suppression of SPFH1 and SPFH2 expression had only slight effects on the turnover of some exogenous model ERAD substrates, and had no effect on sterol-induced ERAD of endogenous 3-hydroxy-3-methylglutaryl-CoA reductase. Overall, these studies show that m3 receptor-expressing HeLa cells are a valuable system for studying IP$_3$ receptor ERAD, and suggest that the SPFH1/2 complex is a factor that selectively mediates the ERAD of activated IP$_3$ receptors.

Introduction

The ubiquitin-proteasome pathway (UPP) provides the primary route for proteolysis within cells and has two parts - the attachment of polyubiquitin chains to selected proteins and the recognition and degradation of these polyubiquitinated proteins by the proteasome, a 26S multi-subunit protease located in the cytosol and nucleus [1]. The endoplasmic reticulum (ER)-associated degradation (ERAD) pathway is a facet of the UPP responsible for the degradation of aberrant proteins in the ER [1]. In addition to this "quality control" function, the ERAD pathway also accounts for the elimination of certain metabolically-regulated native ER membrane proteins, including inositol 1,4,5-trisphosphate (IP$_3$) receptors (IP$_3$Rs) [2] and 3-hydroxy-3-methylglutaryl-CoA reductase (HMGR) [3].

IP$_3$Rs form tetrameric, IP$_3$- and Ca^{2+}-gated Ca^{2+} channels in ER membranes and play a key role in cell signaling [4]. Stimulation of certain cell surface receptors triggers IP$_3$ formation at the plasma membrane, which then diffuses through the cytosol and binds to IP$_3$Rs [4]. This, in concert with Ca^{2+} binding, induces conformational changes in the tetrameric channel that permit Ca^{2+} to flow from stores within the ER lumen into the cytosol [4]. There are three IP$_3$R types in mammals, IP$_3$R1, IP$_3$R2 and IP$_3$R3, and while they differ considerably in their tissue distribution, they have broadly similar properties, are often co-expressed, and can form homo- or heterotetramers [4]. Remarkably, G-protein-coupled receptor (GPCR)-induced activation of endogenous IP$_3$Rs can lead to their rapid polyubiquitination and subsequent degradation by the proteasome [2,5,6], a phenomenon that has been demonstrated in many mammalian cell types, including gonadotropin-releasing hormone-stimulated αT3-1 mouse pituitary gonadotropes [7], and endothelin 1-stimulated Rat-1 primary fibroblasts [8]. The ERAD pathway seems to be responsible for this process, as a ubiquitin-conjugating enzyme that ubiquitinates IP$_3$Rs is Ubc7 [9], an enzyme widely implicated in ERAD [1,3], and the p97-

Ufd1-Npl4 complex, which is known to facilitate the extraction of ERAD substrates from the ER membrane [1,3], also mediates the degradation of polyubiquitinated IP$_3$Rs [10]. Importantly, endogenous IP$_3$Rs represent a unique tool for studying ERAD, since activation almost instantaneously converts them from stable, native proteins into ERAD substrates [2,7, 10].

Here, we sought to establish a HeLa cell-based system for the study of IP$_3$R ERAD, since HeLa cells are very amenable to transient transfection with exogenous constructs, including those that mediate RNA interference [11,12]. To this end, we transfected HeLa cells to stably express m3 muscarinic receptors and found that activation of those muscarinic receptors with carbachol did indeed elicit IP$_3$R ERAD. Further, in seeking to define the proteins that mediate IP$_3$R ERAD we found that two partially-characterized proteins, SPFH1 and SPFH2 (also known as erlin-1 and erlin-2) [13,14], which exist as a heteroligomeric complex, rapidly associate with IP$_3$ receptors in a manner that precedes polyubiquitination, and mediate IP$_3$ receptor ERAD. Our data suggest that the SPFH1/2 complex is a factor that selectively targets activated IP$_3$ receptors for ERAD.

Experimental Procedures

Cells

HeLa cells were cultured in Dulbecco's modified Eagle's medium supplemented with 5% fetal bovine serum, 100 units/mL penicillin and 100 μg/mL streptomycin. mHela cells were prepared by transfecting HeLa cells with a pcDNA3.1+-based plasmid encoding human m3 muscarinic acetylcholine receptor tagged at the N-terminus with 3 hemagglutinin (HA) epitopes (UMR cDNA Resource Center). In brief, 10^5 HeLa cells were transfected with 2μg *Pvu I*-linearized plasmid / 3μl LipoFectamine2000 (Invitrogen), were subcultured into 96-well plates, and were grown for 14-20 days in culture medium containing 1.3mg/ml G418 to obtain single G418-resistant clones. The clone (M4) expressing the highest m3 muscarinic receptor levels (as assessed by HA-epitope immunoreactivity) was selected for further study, was maintained in medium containing 300μg/ml G418, and was subcultured in G418-free medium prior to experiments.

Materials

Antibodies used were: rabbit polyclonal anti-IP$_3$R1 [6], anti-SPFH2 [15] and anti-HMGR membrane region [16], rat monoclonal anti-grp94 (StressGen), and mouse monoclonal anti-ubiquitin clone FK2 (Bio-Mol International) or clone P4D1 (Santa Cruz Biotechnology), anti-HMGR clone A9 (ATCC), anti-β-actin (Sigma), anti-p97 (Research Diagnostics, Inc.), anti-IκBα (BD Transduction Laboratories), anti-GFP (Roche Diagnostics), and anti-SPFH1 (a gift from Dr Stephen Robbins; clone 10E6 being used for immunoprecipitations and clone 7D3 being used for immunoblotting) [13]. Triton X-100, puromycin, cycloheximide (CHX), protease inhibitors, cholesterol, N-ethylmaleimide (NEM), carbachol, and tumor necrosis factor α (TNFα) were purchased from Sigma; MG-132 was from Calbiochem; mevalonate was from Fluka; 25-hydroxycholesterol was from Steraloids; G418 was from Invitrogen; and Protein A-Sepharose CL-4B was from Amersham Biosciences. Bortezomib was a gift from Millennium Pharmaceuticals, and compactin was a gift from Dr Robert Simoni. Lipoprotein-deficient fetal calf serum (LPDS) was prepared as described [17].

IP$_3$R down-regulation and polyubiquitination

For down-regulation experiments (Figure 1B), mHeLa cells were seeded at 5×10^5 cells / well in 6-well plates, were incubated in culture medium with stimuli, were detached with 155mM NaCl, 10mM HEPES, 1mM EDTA, pH 7.4 (HBSE), were centrifuged (16,000 × *g* for 1min at 25°C), were solubilized for 30min at 4°C with ~100μl lysis buffer (150mM NaCl, 50mM

Tris-HCl, 1mM EDTA, 1% Triton X-100, pH 8.0) supplemented with a protease inhibitor cocktail (0.2mM phenylmethylsulfonyl fluoride, 10μM leupeptin, 10μM pepstatin, 0.2μM soybean trypsin inhibitor) and 1mM DTT, were centrifuged (16,000 × g for 10min at 4°C), and samples were mixed with gel loading buffer for electrophoresis and immunoblotting [6, 15]. For polyubiquitination / co-immunoprecipitation experiments (Figures 1C and 2A), confluent monolayers in two 15cm diameter dishes were incubated in culture medium with stimuli and were solubilized by the addition of lysis buffer plus protease inhibitor cocktail. Lysates were then treated with 2.5mM NEM for 1min to inhibit deubiquitinating enzymes, followed by 5mM DTT. After 30min at 4°C, lysates were centrifuged (16,000 × g for 10min at 4°C) and IP$_3$R1 was immunoprecipitated by incubating with anti-IP$_3$R1 and Protein A-Sepharose CL-4B for 6-16h at 4°C. Immunoprecipitates were washed thoroughly with lysis buffer (1,000 × g for 1min at 4°C) and resuspended in gel loading buffer for subsequent electrophoresis and immunoblotting [6, 15].

RNA interference in mHeLa cells

Short interfering RNA (siRNA) sequences against human SPFH2 mRNA (SPFH2si1 and SPFH2si5) and a control siRNA (Random), have been described previously [15]. These and two siRNAs designed against human SPFH1 mRNA, encoded by TCCCAGAAGCCATAAGAAG (SPFH1si2) and GTACCAGGCCATTGCTTCT (SPFH1si4), and which were equally effective, were expressed from pSUPER.retro.puro vectors [15]. To measure effects of RNA interference on IP$_3$R1 and HMGR down-regulation, IP$_3$R1 polyubiquitination, or IκBα processing, mHeLa cells were seeded, respectively, in 6-well plates (2×10^5 / well), 10cm diameter dishes (12×10^6 / dish) or 12-well plates (10^5 / well) in antibiotic-free medium, and 24h later were transiently transfected using LipoFectamine2000 and pSUPER.retro.puro vectors in the ratios 6μl / 2.4μg, 34μl / 14μg, and 3μl / 1.2μg. After 24h, the medium was replaced with medium supplemented with puromycin (1μg/ml) to kill non-transfected cells, 24h later medium was changed, and 24h later cells were stimulated and lysates were prepared and processed as already indicated. To facilitate HMGR analysis (Fig 7A), this enzyme was up-regulated prior to cell stimulation by incubation for 24h in medium supplemented with 5% (v/v) LPDS, 2μM compactin and 100μM mevalonate [17]. In restoration experiments (Fig 4A, lanes 6-9), cells were transfected 24h prior to stimulation with a mouse SPFH2 cDNA construct (SPFH2-5*; 34μl LipoFectamine2000 / 14μg cDNA) that contains silent mutations that render the mRNA resistant to SPFH2si5 [15].

Calcium measurements

Cytosolic Ca^{2+} concentration in cell suspensions was measured by loading cells with 10μM Fura2-AM for 30min at 37°C as described [8]. Imaging of adherent single cells was achieved using a Till Photonics Polychrome V to generate 340 and 380nm light, an Olympus IX71 inverted microscope fitted with a UApo/340, 40×, 1.35 numerical aperture oil immersion objective, an Imago-QE camera to capture images, and Tillvision software to run experiments. Cells (2×10^5) on 25mm glass cover slips were rinsed three times and incubated in Krebs-HEPES buffer [8] with 5μM Fura2-AM for 45min at 37°C, were rinsed three times, were incubated for 10min at 37°C, and finally were perfused on the microscope stage at 37°C with Krebs-HEPES buffer.

Analysis of model ERAD substrates

GFPu is an unstable variant of EGFP created by fusing the CL1 degron to its C-terminus [18]. The other substrates used were TCRα, a transmembrane subunit of the T-cell receptor complex [19], and two terminally misfolded, ER luminal proteins, the glycosylated null Hong Kong variant of α$_1$-antitrypsin (A1AT-NHK) [20] and the nonglycosylated transthyretin D18G mutant (TTR-D18G) [21]. GFP tags were added by fusing EGFP cDNA to the 3′ end of

substrate cDNAs and insertion into pcDNA3.1+ as described [22]. HEK cells stably expressing GFPu, TCRα-GFP, A1AT-NHK-GFP or TTR-D18G-GFP [22] were transiently transfected using Fugene 6 (Roche) with pSUPERSTAR constructs encoding SPFH1si2 and SPFH2si5, or siRNAs against S2, or Hrd1 (encoded by GAAACATTATTCTAGGCAA and GAGACAGTTTCAGATGATT, respectively). The constructs also encode a truncated CD4 cell surface marker to facilitate detection and analysis of transfected cells [22]. 72 h later, cells in suspension were labeled with allophycocyanin-conjugated anti-CD4 (Invitrogen), and a FACSCalibur flow cytometer (Becton Dickson) was employed to measure GFP fluorescence levels for ~20,000 CD4+ cells as previously described [22]. Mean GFP fluorescence in CD4 + cells was determined and normalized to the levels in Random shRNA-expressing cells for three independent experiments. The turnover of these substrates in HeLa cells was examined by transiently co-transfecting cells in 24-well plates (plated 24 h earlier at 5×10^4 cells/well) with cDNAs encoding the GFP-tagged substrates in pcDNA3.1+ together with SPFH1si4 plus SPFH2si7 (encoded by GTACAAGGCCATTGCTTCC) in $6OH_1OpSUPER.retro.puro$, selecting for shRNA-expressing cells with 1 μg/mL puromycin, and 72 h later, measuring substrate levels with anti-GFP as described [15].

Analysis of HMGR processing

Random or SPFH1si4 plus SPFH2si6 siRNAs were expressed in Rat1 cells from the doxycycline-regulated $6OH_1O$-pSUPER.retro.puro vector as described [23]. Endogenous HMGR levels were upregulated by incubating the cells for 12-16h in DMEM supplemented with 10% (v/v) LPDS, 2μM compactin and 100μM mevalonate. Metabolic labeling with [^{35}S]-methionine/cysteine, immunoprecipitation, and immunoprobing for polyubiquitinated HMGR or unmodified HMGR were carried out as previously described [16,24,25].

Data presentation and analysis

All experiments were repeated at least once, and representative images of gels, micrographs or Ca^{2+} traces are shown. Immunoreactivity was quantitated using a Genegnome Imager (Syngene BioImaging) and are graphed as mean ± SEM of n independent experiments. Routinely (e.g. for SPFH2), quantitation was of discrete bands of a specific size, while for polyubiquitinated IP_3R1, ubiquitin immunoreactivity in the 270-380kDa region of gels was assessed.

Results

IP_3R1 processing in mHeLa cells

mHela cells were prepared by stable transfection of HeLa cells with a vector encoding HA-tagged human m3-muscarinic receptor. Exposure of mHela cells to the muscarinic receptor agonist carbachol caused a rapid and sustained elevation of cytosolic Ca^{2+} concentration that was not seen in unmodified HeLa cells (Figure 1A), indicating that the exogenous m3 receptors couple appropriately to IP_3 production, IP_3R activation and Ca^{2+} mobilization [4].

The experimental hallmarks of GPCR-induced IP_3R ERAD are that proteasome inhibitors block IP_3R degradation, and that in the absence of proteasome inhibitors, only a small fraction of IP_3Rs (<10%) can be seen to be polyubiquitinated, because polyubiquitinated IP_3Rs are rapidly degraded by the proteasome [2,7]. This was the case in carbachol-stimulated mHeLa cells. Figure 1B shows that IP_3R1 was down-regulated ~50% by carbachol treatment of mHeLa cells with half-maximal effect at ~1.5h (lanes 3-7). This effect was blocked by the proteasome inhibitor bortezomib (lanes 8-12), and was not seen in unmodified HeLa cells (lanes 1-2). Similar results were seen for IP_3R3 (not shown), which together with IP_3R1, makes up the vast majority of the IP_3R complement of HeLa cells [26], and mHeLa cells (not shown). Fig 1C upper panel shows that in mHeLa cells (lanes 3-10), but not in unmodified HeLa cells (lanes

1-2), carbachol increased IP_3R1 polyubiquitination, peaking at ~20min. That IP_3R1 immunoreactivity (lower panel) was not clearly smeared upwards is consistent with only a small fraction of IP_3Rs being polyubiquitinated. Figure 1C also shows that carbachol-induced IP_3R1 polyubiquitination was blocked by co-incubation with the muscarinic receptor antagonist atropine (lane 12), indicating that the effects of carbachol are mediated by the exogenous m3 receptors. Likewise, thapsigargin, which inhibits ER Ca^{2+}-ATPase and depletes ER Ca^{2+} stores in HeLa cells [26], was inhibitory (lane 11). This is also a hallmark of IP_3R ERAD, presumably because intact Ca^{2+} stores are needed for the events that trigger IP_3R polyubiquitination [10]. Overall, these data show that the processing of IP_3Rs in mHeLa cells is essentially identical to that seen in other cells types in which endogenous GPCRs are used to initiate IP_3R ERAD. It is interesting to note, however, that under resting conditions, IP_3R1 levels in mHeLa cells were less than that seen in HeLa cells (Fig 1B, compare lanes 1 and 3) and IP_3R1 polyubiquitination was slightly more pronounced (Figure 1C, compare lanes 1 and 3). This suggests that some IP_3R ERAD may be occurring in resting mHeLa cells, perhaps because the exogenous muscarinic receptors can slightly elevate basal IP_3 levels even in the absence of stimulus.

SPFH1 and SPFH2 associate with activated IP_3Rs

The known capacity of proteins that mediate ERAD (e.g. p97) to associate with activated IP_3Rs in αT3-1 and Rat 1 cells [8,15,23], motivated us to examine whether p97, and perhaps additional mediators, might associate with activated IP_3Rs in mHeLa cells. To study the association dynamics of these proteins with activated IP_3R1, we stimulated mHeLa cells with carbachol for various times, immunoprecipitated IP_3R1, and probed immunoblots for a variety of proteins (Fig. 2A). p97 co-immunoprecipitated with IP_3R1 in a manner that slightly lagged behind IP_3R1 polyubiquitination, peaking at 20-30min. As p97, and its cofactors Ufd1 and Npl4, directly bind to ubiquitin [1,3,27], this interaction of p97 with activated IP_3Rs could well be via attached ubiquitin moieties. We also probed for SPFH1 and SPFH2. These ~340 amino acid proteins are closely related (73% identical and 91% similar) [13,14,23] and share homology with a diverse family of proteins that contain an SPFH domain, an ~200 amino acid motif of unknown function, named for the original family members: Stomatin, Prohibitin, Flotillin, and HflC/HflK [14]. Interestingly, SPFH1 and SPFH2 have also recently been reported to be components of detergent-resistant membranes derived from the ER [13] and to associate with IP_3Rs in stimulated αT3-1 and Rat-1 cells [15,23]. In mHeLa cells, the peak interaction of SPFH1 and SPFH2 with IP_3R1 occurred prior to peak polyubiquitination, and both were strongly associated with IP_3R1 as little as 1min after carbachol addition (Fig 2A). Fig 2B verifies that anti-SPFH1 and anti-SPFH2 are specific to their intended targets, recognizing proteins at ~41kDa and ~43kDa, respectively. Probing for grp94 served as a negative control; this ER luminal protein did not co-immunoprecipitate with IP_3R1 at all after carbachol addition (Fig 2A).

It has recently been shown that SPFH1 and SPFH2 associate into hetero-oligomeric ~1MDa complexes [23,28]. This was also the case in mHeLa cells, since both proteins migrated at ~1MDa under non-denaturing conditions (Fig 3A, lanes 1 and 2), and anti-SPFH2 immunoprecipitated and immunodepleted both SPFH2 and SPFH1 from cell lysates (Fig 3B, lane 3), as did anti-SPFH1 (lane 2), albeit less effectively than anti-SPFH2, due to anti-SPFH1 being relatively ineffective at immunoprecipitating. Overall, these data indicate that in mHeLa cells, a complex composed of SPFH1 and SPFH2 binds to IP_3R1s as soon as they are activated and prior to their polyubiquitination.

RNA interference of SPFH1 and / or 2 inhibits IP_3R processing

In order to investigate the roles of SPFH1 and SPFH2 we used RNA interference to "knock down" each protein. On average (n=6), SPFH1 siRNA reduced SPFH1 immunoreactivity by

87±2% without inhibiting SPFH2 levels (e.g. Figure 4B, lane 4), while SPFH2 siRNA reduced SPFH2 immunoreactivity by 80±5% and surprisingly also reduced SPFH1 immunoreactivity by 40±6% (e.g. Figure 4B, lane 7). When the siRNAs were combined, SPFH1 and SPFH2 immunoreactivities were reduced by 88±2% and 78±6%, respectively (e.g. Figure 4B, lane 10). Why the SPFH2 siRNA also affects SPFH1 levels is presently unclear, but maybe because it weakly targets SPFH1 mRNA. SPFH2 siRNA strongly inhibited carbachol-induced IP_3R1 polyubiquitination (Figure 4A, lane 4) and down-regulation (Figure 4B, lanes 7-9) and clearly elevated resting IP_3R1 levels (Figure 4B, compare lanes 1 and 7). SPFH1 siRNA had similar but less pronounced effects on IP_3R1 polyubiquitination (Figure 4A, lane 3) and down-regulation (Figure 4B, lanes 4-6), and the siRNAs in combination were not substantially more effective than SPFH2 siRNA alone (Figure 4A, lane 5 and Figure 4B, lanes 10-12). Overall, these data are consistent with recent studies in Rat1 cells in which both SPFH1 and SPFH2 siRNAs strongly inhibited IP_3R1 processing [23]. The greater effectiveness of SPFH2 siRNA seen in the present study likely results from the fact that, in mHeLa cells, SPFH2 siRNA depletes both SPFH1 and SPFH2, while SPFH1 siRNA depletes only SPFH1. Intriguingly, SPFH1 knockdown reduced co-immunoprecipitation of SPFH2 with IP_3R1 (Figure 4A, lane 3), and vice versa (lane 4), indicating again that it is the complex formed by these proteins that binds to activated IP_3Rs. Importantly, the data shown in Figure 4 could be replicated when siRNAs targeting other SPFH1 and SPFH2 mRNA sequences were used (data not shown), indicating that "off-target" effects are not responsible for the inhibition of IP_3R1 processing. Further, reintroduction of exogenous SPFH2 by transient transfection into mHeLa cells in which endogenous SPFH2 was depleted by RNA interference partially reversed inhibition of IP_3R1 polyubiquitination (Figure 4A, lanes 6-9); most likely the restoration is incomplete because transient transfection does not cause the expression of exogenous SPFH2 in all cells (data not shown). Overall, since knockdown of SPFH1 and / or SPFH2 inhibits IP_3R1 polyubiquitination, it appears that the complex formed by these proteins somehow mediates this event. As IP_3R polyubiquitination requires that IP_3Rs can be activated normally [10] it is a formal possibility that the inhibitory effect of SPFH1 and / or SPFH2 knockdown could result from inhibition of IP_3R activation. However, this was not the case, as Ca^{2+} mobilization in response to carbachol was unaffected by SPFH1 and 2 knockdown (Fig. 5A).

To further examine the specificity of the functions of the SPFH1/2 complex, we examined the processing of IκBα, a cytosolic protein that is rapidly degraded via the UPP, but independently of ERAD [29]. In HeLa cells, TNFα has been shown previously to stimulate IκBα polyubiquitination and degradation, with proteasome inhibitors causing the accumulation of polyubiquitinated species and blocking IκBα degradation [29,30]. These events were not inhibited by SPFH1 and 2 knockdown in mHeLa cells (Fig. 5B, compare lanes 3 and 4, with 9 and 10). Remarkably, muscarinic receptor activation also caused IκBα polyubiquitination and degradation, albeit to a lesser extent than TNFα. Again, however, this was not affected by SPFH1 and 2 knockdown (Figure 5B, compare lanes 5 and 6, with 11 and 12). Graphing the time course of IκBα degradation (Figure 5C) confirmed the lack of effect of SPFH1 and 2 knockdown, but also revealed that SPFH1 and 2 knockdown caused a slight (~10%) reduction in IκBα levels, even in the absence of stimulus, the reason for which is presently unclear. Overall, Fig 5 shows that the inhibitory effects of SPFH1 and 2 knockdown on IP_3R processing in mHeLa cells are not due to a general perturbation of the UPP or inhibition of m3 receptor function.

Effects of SPFH1 and SPFH2 knockdown on the stability of model ERAD substrates and HMGR

To examine whether the SPFH1/2 complex is specific for IP_3Rs, or plays a more general role in ERAD, we initially assessed the effects of SPFH1 and SPFH2 depletion on the degradation of several GFP-tagged "model" ERAD substrates: TCRα [19], A1AT-NHK [20] and TTR-

D18G [21]. Steady-state GFP fluorescence in cells expressing these proteins reflects the balance between the their synthesis and degradation, and a degradation defect results in increased GFP fluorescence, which can be readily measured by flow cytometry [22]. Depletion of SPFH1 and SPFH2 in HEK cells had a slight but significant effect on the steady-state levels of A1AT-NHK-GFP and TTR-D18G-GFP, but not of TCRα-GFP or GFPu, a cytosolic UPP substrate (Fig. 6A) [18]. In contrast, depletion of the ERAD ubiquitin ligase Hrd1 [3] or the S2 subunit of the proteasome [1] stabilized all four substrates, albeit to different extents, indicating that they have different processing requirements. Knockdown of SPFH1 and SPFH2 also slightly increased the basal levels of A1AT-NHK-GFP and TTR-D18G-GFP (but not TCRα-GFP) when expressed in HeLa cells (Fig. 6B), and slightly inhibited their degradation rates measured after CHX addition (Fig. 6B). Thus, the SPFH1/2 complex regulates the stability of certain ERAD substrates (A1AT-NHK-GFP and TTR-D18G-GFP), although the effect of SPFH1/2 depletion on these substrates is less pronounced than that seen for activated IP$_3$Rs (Fig 4B, lowest panel). Possible explanations for this difference are that the SPFH1/2 complexes that remain after RNAi are better able to support the ERAD of exogenous model substrates than endogenous IP$_3$Rs, or that exogenous model substrates can undergo degradation via multiple routes, only one of which is mediated by the SPFH1/2 complex.

Finally, we examined whether sterol-induced ERAD of HMGR [3,25] in mHeLa cells requires SPFH1 and 2 (Figure 7A). Sterols effectively down-regulated HMGR levels, but this was unaffected by SPFH1 and 2 knockdown (lanes 1-6, and graph i), while under exactly the same experimental conditions, carbachol-induced IP$_3$R1 down-regulation was blocked by SPFH1 and 2 knockdown (lanes 7-12, and graph iv). Additional controls showed that sterols did not cause IP$_3$R1 down-regulation (lanes 1-6 and graph iii) and that carbachol did not cause HMGR down-regulation (lanes 7-12 and graph ii). Thus, SPFH1 and 2 do not mediate sterol-induced HMGR ERAD in mHeLa cells. We also examined Rat1 cells in which we have found sterols to cause a profound increase in endogenous HMGR ubiquitination (Fig 7B) and degradation (Fig 7C), and in which SPFH1 and 2 can be effectively depleted by RNA interference (Fig 7B, lowest panels). However, sterol-induced HMGR ubiquitination (Fig 7B) and degradation (Fig 7C) were unaffected by SPFH1 and 2 depletion, confirming that the SPFH1/2 complex is not involved in HMGR processing. In contrast, in these same cells, SPFH1 and 2 depletion almost completely blocks the ERAD of activated IP$_3$Rs [23].

Discussion

The mechanism by which activated IP$_3$Rs are degraded by the ERAD pathway remains largely undefined. We have begun to identify the proteins that mediate this process using virally transduced Rat-1 cell cultures stably expressing exogenous siRNAs [8,15,23], but more rapid screening of siRNAs has been hampered by the fact that Rat-1 cells exhibit low transfection efficiency in transient transfection studies [8]. To accelerate this work we sought a cell line in which IP$_3$R ERAD can be measured that is also amenable to transient transfection with siRNA-expressing vectors, and chose to use HeLa cells, since these cells are known to be excellent recipients of transiently-introduced siRNAs [11,12]. However, preliminary studies (not shown) demonstrated that none of the endogenous GPCRs in Hela cells were capable of eliciting IP$_3$R ERAD, and thus we chose to introduce m3 muscarinic receptors, since these have been shown to initiate IP$_3$R ERAD in other cell types [31]. We found that introduction of m3 receptors allowed for robust carbachol-induced increases in cytosolic Ca^{2+} concentration, IP$_3$R1 polyubiquitination and IP$_3$R1 down-regulation with characteristics similar to that seen in other cell types.

Carbachol also caused the rapid association of SPFH1 and SPFH2 with activated IP$_3$Rs, and the less rapid association of p97. SPFH1 and SPFH2 are closely related proteins, that contain an N-terminal transmembrane domain that targets the proteins to the ER membrane and a C-

terminal region, including the SPFH domain, in the ER lumen [13-15,23,28]. Intriguingly, SPFH domain-containing proteins are often found in large oligomeric structures [14], and this has recently also been shown to be the case for SPFH1 and 2 [23,28]. mHeLa cell SPFH1 and 2 were also found in high molecular mass complexes, and it seems very likely that it is these complexes that are associating with activated IP$_3$Rs.

Knockdown of SPFH1 and / or SPFH2 in mHeLa cells inhibited carbachol-induced IP$_3$R1 polyubiquitination and down-regulation and also elevated basal IP$_3$R1 levels, pointing towards a role for the SPFH1/2 complex in IP$_3$R processing. Importantly, SPFH1 and 2 knockdown did not affect Ca^{2+} signaling via IP$_3$Rs, demonstrating that the locus of action of the complex is down-stream of IP$_3$R activation. These findings are consistent with those from virally transduced Rat-1 cell cultures in which SPFH1 and 2 knockdown also inhibited IP$_3$R polyubiquitination and down-regulation [23]. This leads us to speculate that the SPFH1/2 complex is a factor that recognizes activated IP$_3$Rs as potential ERAD substrates and triggers their polyubiquitination. The recognition site could be the large intraluminal loop between the fifth and sixth transmembrane domains of IP$_3$Rs [4], since the bulk of SPFH1 and 2 appear to reside in the ER lumen [13-15,23], and this loop is already known to mediate interactions between IP$_3$R1 and other proteins [4].

Is the SPFH1/2 complex a specific mediator of IP$_3$R ERAD, or does it have a more general role in ERAD? Support for the latter viewpoint has come from studies showing that certain ERAD pathway components (e.g. p97 and derlin1) co-purify with the SPFH1/2 complex [15], and that certain exogenous model ERAD substrates (e.g. CD3δ) are slightly stabilized by SPFH2 knockdown [15]. Additionally, SPFH1 and SPFH2 bind to certain proteins undergoing ERAD, including CFTRΔF508 [32] and the α$_{1D}$-adrenergic receptor [33]. However, the data shown herein indicate that not all ERAD substrates are affected by SPFH1 and SPFH2 knockdown, and that those that are affected (A1AT-NHK-GFP and TTR-D18G-GFP), are stabilized only slightly and much less than that seen after knockdown of Hrd1 or the S2 proteasome subunit, which are key ERAD pathway components [1,3]. This indicates that the SPFH1/2 complex is not a central component of the mammalian ERAD pathway. Further, sterol-induced ubiquitination and degradation of endogenous HMGR is completely unaffected by knockdown of SPFH1 and SPFH2, showing that the processing of this substrate, which requires recognition by INSIGs [3], does not involve the SPFH1/2 complex. Thus, while the SPFH1/2 complex is required for IP$_3$R ERAD and contributes slightly to the degradation of certain model ERAD substrates, it is not essential for the processing of all ERAD substrates in mammalian cells, and is most likely an ERAD recognition factor with selectivity towards activated IP$_3$Rs.

In summary, we have developed a HeLa cell line (mHeLa cells) in which it is possible to study IP$_3$R ERAD and have found, using immunoprecipitation and RNAi, that the SPFH1/2 complex mediates this process. The amenability of these cells to RNAi screening and protein over-expression [12] should greatly facilitate examination of the proteins that mediate IP$_3$R ERAD.

Acknowledgments

Literature Cited

1. Vembar SS, Brodsky JL. One step at a time: Endoplasmic reticulum-associated degradation. Nat Rev Mol Cell Biol 2008;9:944–957. [PubMed: 19002207]

2. Wojcikiewicz RJH, Pearce MMP, Sliter DA, Wang Y. When worlds collide: IP$_3$ receptors and the ERAD pathway. Cell Calcium 2009;46:147–153. [PubMed: 19709743]

3. Hampton RY, Garza RM. Protein quality control as a strategy for cellular regulation: lessons from ubiquitin-mediated regulation of the sterol pathway. Chem Rev. 2009in press

4. Foskett JK, White C, Cheung KH, Mak DD. Inositol trisphosphate receptor Ca^{2+} release channels. Physiol Rev 2007;87:593–658. [PubMed: 17429043]

5. Bokkala S, Joseph SK. Angiotensin II-induced down-regulation of inositol trisphosphate receptors in WB rat liver epithelial cells. Evidence for involvement of the proteasome pathway. J Biol Chem 1997;272:12454–12461. [PubMed: 9139693]

6. Oberdorf J, Webster JM, Zhu CC, Luo SG, Wojcikiewicz RJ. Down-regulation of types I, II and III inositol 1,4,5-trisphosphate receptors is mediated by the ubiquitin/proteasome pathway. Biochem J 1999;339:453–461. [PubMed: 10191279]

7. Wojcikiewicz RJH, Xu Q, Webster JM, Alzayady K, Gao C. Ubiquitination and proteasomal degradation of endogenous and exogenous inositol 1,4,5-trisphosphate receptors in alpha T3-1 anterior pituitary cells. J Biol Chem 2003;278:940–947. [PubMed: 12421829]

8. Alzayady KJ, Panning MM, Kelley GG, Wojcikiewicz RJH. Involvement of the p97-Ufd1-Npl4 complex in the regulated endoplasmic reticulum-associated degradation of inositol 1,4,5-trisphosphate receptors. J Biol Chem 2005;280:34530–34537. [PubMed: 16103111]

9. Webster JM, Tiwari S, Weissman AM, Wojcikiewicz RJH. Inositol 1,4,5-trisphosphate receptor ubiquitination is mediated by mammalian Ubc7, a component of the endoplasmic reticulum-associated degradation pathway, and is inhibited by chelation of intracellular Zn^{2+} J Biol Chem 2003;278:38238–38246. [PubMed: 12869571]

10. Alzayady KJ, Wojcikiewicz RJH. The role of Ca^{2+} in triggering inositol 1,4,5-trisphosphate receptor ubiquitination. Biochem J 2005;392:601–606. [PubMed: 16134970]

11. Hattori M, Suzuki AZ, Higo T, Miyauchi H, Michikawa T, Nakamura T, Inoue T, Mikoshiba K. Distinct Roles of Inositol 1,4,5-Trisphosphate Receptor Types 1 and 3 in Ca2+ Signaling. J Biol Chem 2004;279:11967–11975. [PubMed: 14707143]

12. Wojcik C, Fabunmi R, DeMartino GN. Modulation of gene expression by RNAi. Methods in Molecular Medicine 2005;108:381–393. [PubMed: 16028696]

13. Browman DT, Resek ME, Zajchowski LD, Robbins SM. Erlin-1 and erlin-2 are novel members of the prohibitin family of proteins that define lipid-raft-like domains of the ER. J Cell Sci 2006;119:3149–3160. [PubMed: 16835267]

14. Browman DT, Hoegg MB, Robbins SM. The SPFH domain-containing proteins: More than lipid raft markers. Trends Cell Biol 2007;17:394–402. [PubMed: 17766116]

15. Pearce MMP, Wang Y, Kelley GG, Wojcikiewicz RJH. SPFH2 mediates the endoplasmic reticulum-associated degradation of inositol 1,4,5-trisphosphate receptors and other substrates in mammalian cells. J Biol Chem 2007;282:20104–20115. [PubMed: 17502376]

16. Roitelman J, Olender EH, Bar-Nun S, Dunn WA Jr, Simoni RD. Immunological evidence for eight spans in the membrane domain of 3-hydroxy-3-methylglutaryl coenzyme A reductase: implications for enzyme degradation in the endoplasmic reticulum. J Cell Biol 1992;117:959–973. [PubMed: 1374417]

17. Goldstein JL, Basu SK, Brown MS. Receptor-mediated endocytosis of low-density lipoprotein in cultured cells. Methods Enzymol 1983;98:241–260. [PubMed: 6321901]

18. Bence NF, Sampat RM, Kopito RR. Impairment of the ubiquitin-proteasome system by protein aggregation. Science 2001;292:1552–1555. [PubMed: 11375494]

19. Yu H, Kopito RR. The role of multiubiquitination in dislocation and degradation of the alpha subunit of the T cell antigen receptor. J Biol Chem 1999;274:36852–36858. [PubMed: 10601236]

20. Sifers RN, Brashears-Macatee S, Kidd VJ, Muensch H, Woo SL. A frameshift mutation results in a truncated alpha1-antitrypsin that is retained within the rough endoplasmic reticulum. J Biol Chem 1988;263:7330–7335. [PubMed: 3259232]

21. Sekijima Y, Wiseman RL, Matteson J, Hammarström P, Miller SR, Sawkar AR, Balch WE, Kelly JW. The biological and chemical basis for tissue-selective amyloid disease. Cell 2005;121:73–85. [PubMed: 15820680]

22. DeLaBarre B, Christianson JC, Kopito RR, Brunger AT. Central pore residues mediate the p97/VCP activity required for ERAD. Mol Cell 2006;22:451–462. [PubMed: 16713576]

23. Pearce MMP, Wormer DB, Wilkens S, Wojcikiewicz RJH. An ER membrane complex composed of SPFH1 and SPFH2 mediates the ER-associated degradation of IP3 receptors. J Biol Chem 2009;284:10433–10445. [PubMed: 19240031]

24. Roitelman J, Simoni RD. Distinct sterol and nonsterol signals for the regulated degradation of 3-hydroxy-3-methylglutaryl-CoA reductase. J Biol Chem 1992;267:25264–25273. [PubMed: 1460026]

25. Ravid T, Doolman R, Avner R, Harats D, Roitelman J. The ubiquitin-proteasome pathway mediates the regulated degradation of mammalian 3-Hydroxy-3-methylglutaryl-coenzyme A reductase. J Biol Chem 2000;275:35840–35847. [PubMed: 10964918]

26. Matsu-ura T, Michikawa T, Inoue T, Miyawaki A, Yoshida M, Mikoshiba K. Cytosolic inositol 1,4,5-trisphosphate dynamics during intracellular calcium oscillations in living cells. J Cell Biol 2006;173:755–765. [PubMed: 16754959]

27. Ye Y, Meyer HH, Rapoport TA. Function of the p97-Ufd1-Npl4 complex in retrotranslocation from the ER to the cytosol: Dual recognition of nonubiquitinated polypeptide segments and polyubiquitin chains. J Cell Biol 2003;162:71–84. [PubMed: 12847084]

28. Hoegg MB, Browman DT, Resek ME, Robbins SM. Distinct regions within the erlins are required for oligomerization and association with high molecular weight complexes. J Biol Chem 2009;284:7766–7776. [PubMed: 19131330]

29. Alkalay I, Yaron A, Hatzubai A, Orian A, Ciechanover A, Ben-Neriah Y. Stimulus-dependent IκBα phosphorylation marks the NF-κB inhibitor for degradation via the ubiquitin-proteasome pathway. Proc Natl Acad Sci USA 1995;92:10599–10603. [PubMed: 7479848]

30. Xu Q, Farah M, Webster JM, Wojcikiewicz RJH. Bortezomib rapidly suppresses ubiquitin thiolesterification to ubiquitin-conjugating enzymes and inhibits ubiquitination of histones and type I inositol 1,4,5-trisphosphate receptor. Mol Cancer Ther 2004;3:1263–1269. [PubMed: 15486193]

31. Wojcikiewicz RJ, Furuichi T, Nakade S, Mikoshiba K, Nahorski SR. Muscarinic receptor activation down-regulates the type I inositol 1,4,5- trisphosphate receptor by accelerating its degradation. J Biol Chem 1994;269:7963–7969. [PubMed: 8132516]

32. Wang X, Venable J, LaPointe P, Hutt DM, Koulov AV, Coppinger J, Gurkan C, Kellner W, Matteson J, Plutner H, Riordan JR, Kelly JW, Yates JR Iii, Balch WE. Hsp90 cochaperone Aha1 downregulation rescues misfolding of CFTR in cystic fibrosis. Cell 2006;127:803–815. [PubMed: 17110338]

33. Lyssand JS, DeFino MC, Tang XB, Hertz AL, Feller DB, Wacker JL, Adams ME, Hague C. Blood pressure is regulated by an α1D-adrenergic receptor/dystrophin signalosome. J Biol Chem 2008;283:18792–18800. [PubMed: 18468998]

34. Sliter DA, Kubota K, Kirkpatrick DS, Alzayady KJ, Gygi SP, Wojcikiewicz RJH. Mass spectrometric analysis of type 1 inositol 1,4,5-trisphosphate receptor ubiquitination. J Biol Chem 2008;283:35319–35328. [PubMed: 18955483]
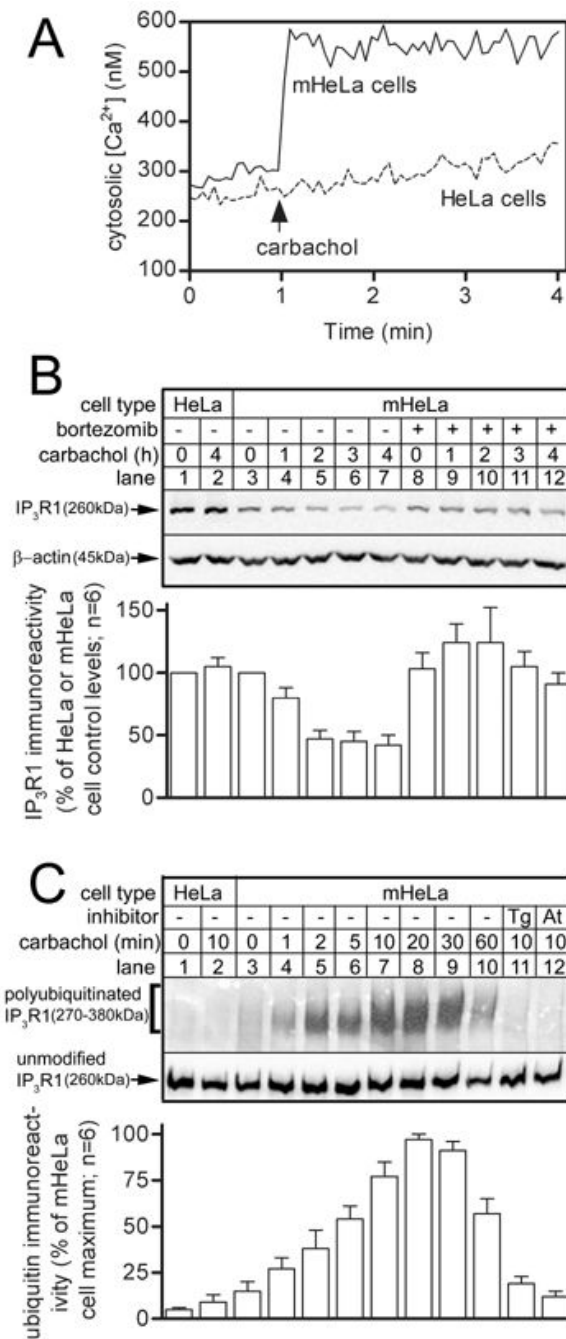
Figure 1. Characteristics of Ca^{2+} signaling and IP$_3$R1 processing in mHeLa cells
A, Suspensions of HeLa and mHeLa cells were exposed to 1mM carbachol as indicated, and cytosolic [Ca^{2+}] was determined. *B*, Monolayers of HeLa and mHeLa cells were incubated as indicated with 10μM carbachol for 1-4h, without or with 1h preincubation with 10μM bortezomib, lysates were prepared, and were probed in immunoblots for IP$_3$R1 and β-actin. *C*, Monolayers of HeLa and mHeLa cells were incubated as indicated with 10μM carbachol in the absence or presence of 1μM thapsigargin (Tg) or 1μM atropine (At), lysates were prepared, and were incubated with anti-IP$_3$R1, and immunoprecipitates were probed for ubiquitin (upper panel) and IP$_3$R1 (lower panel).
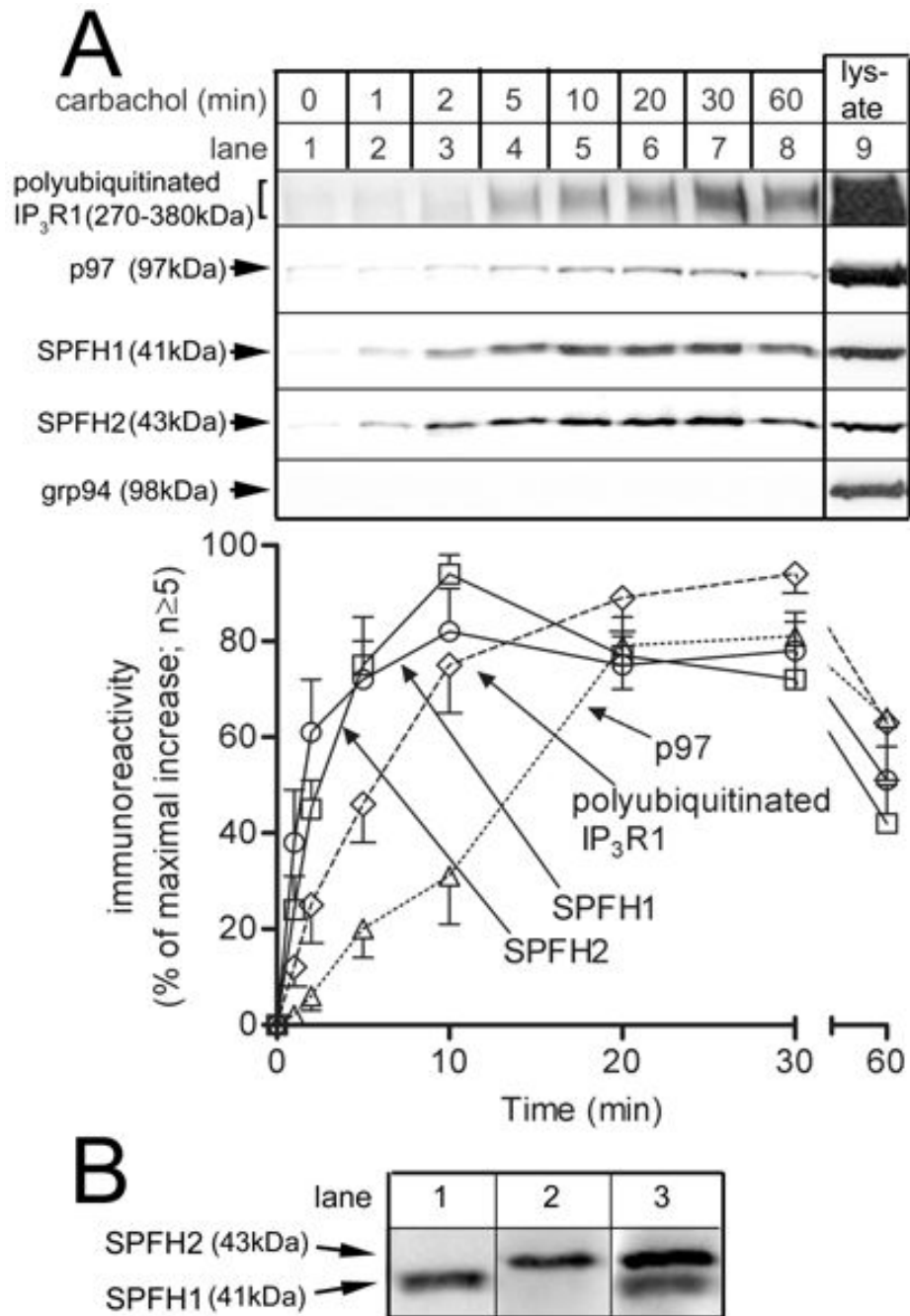
Figure 2. SPFH1 and SPFH2 rapidly associate with activated IP$_3$Rs

A, Monolayers of mHeLa cells were treated with 10μM carbachol for the times indicated, lysates were incubated with anti-IP$_3$R1, and immunoprecipitates were probed for ubiquitin, p97, SPFH1, SPFH2 and grp94 (lanes 1-8) together with cell lysate (lane 9). *B*, mHeLa cell lysates were probed with anti-SPFH1 (lane 1), anti-SPFH2 (lane 2), or with both antisera together (lane 3).
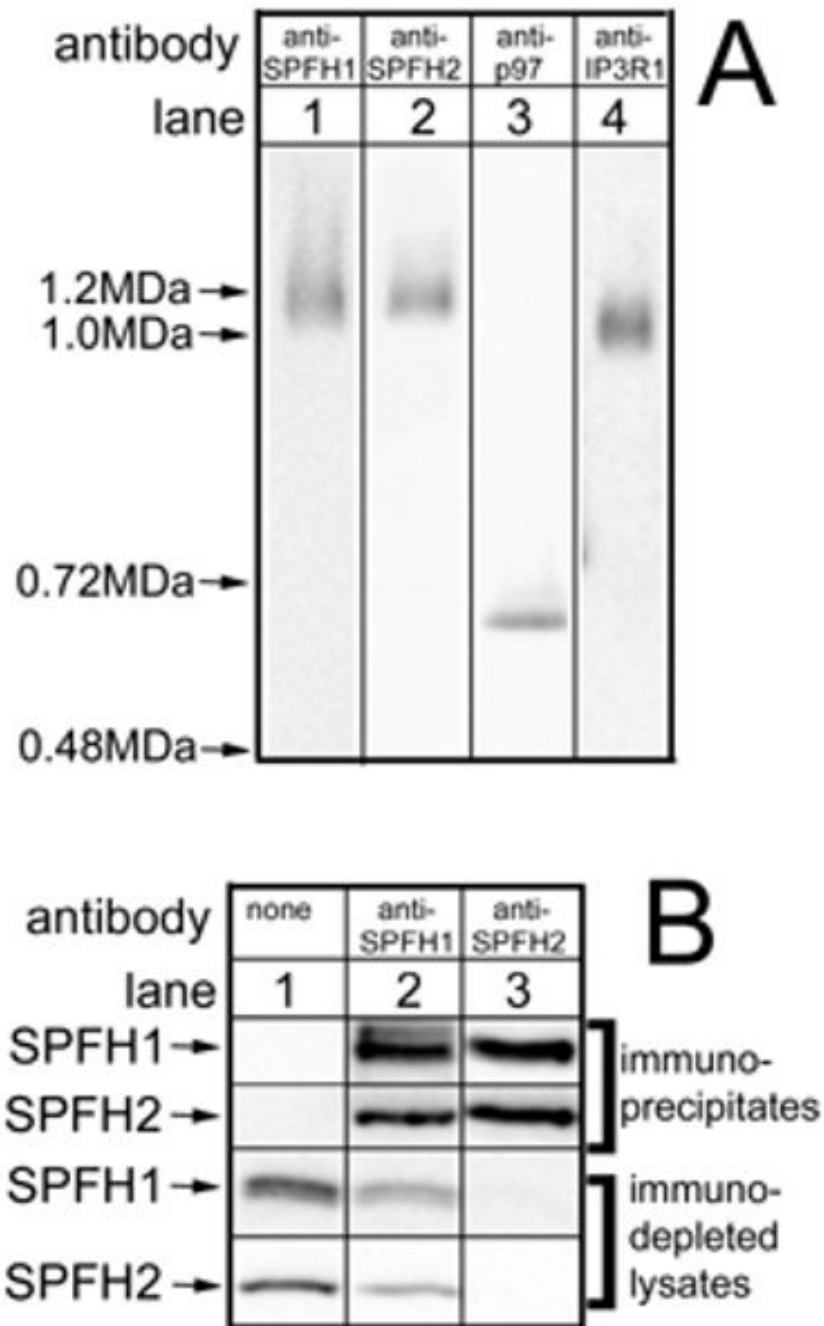
Figure 3. SPFH1 and SPFH2 form a high molecular mass complex
A. mHela cell lysates were subjected to blue-native PAGE as described [34] and were probed with the antibodies indicated. The molecular mass markers and the migration positions of p97 and IP$_3$R1 (which are hexameric and tetrameric, respectively) indicate that SPFH1 and SPFH2 form a large complex. *B*. mHela cell lysates were incubated without antibody (lane 1), or with anti-SPFH1 (lane 2), or anti-SPFH2 (lane 3) and immunoprecipitates and the immunodepleted cell lysates were probed for SPFH1 and SPFH2.
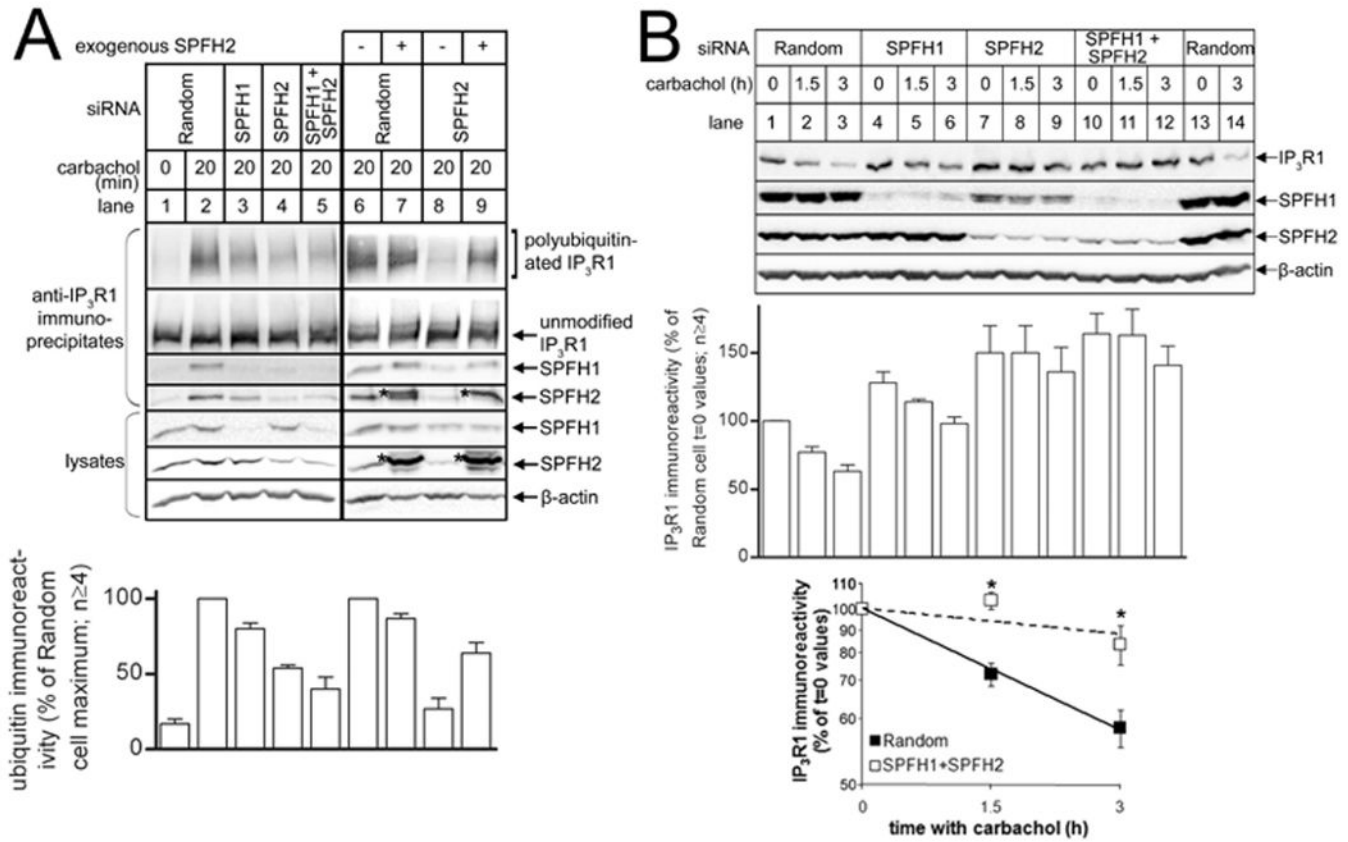
Figure 4. SPFH1 and / or SPFH2 knockdown inhibits the polyubiquitination and degradation of IP$_3$Rs

A. mHeLa cells were transfected with vectors encoding either Random siRNA (lanes 1, 2, 6 and 7), or SPFH1si2 and / or SPFH2si1 plus SPFH2si5 siRNAs (lanes 3-5), or SPFH2si5 siRNA only (lanes 8-9) and 72h later were incubated without or with 10μM carbachol for the times indicated. In restoration experiments (lanes 6-9), cells were transfected 24h prior to carbachol treatment with either empty vector or a construct encoding exogenous SPFH2. Cell lysates were then prepared and were incubated with anti-IP$_3$R1, and immunoprecipitates were probed for ubiquitin, IP$_3$R1, SPFH1 and SPFH2 (upper panels). Cell lysates were also probed for SPFH1, SPFH2 and β-actin (lower panels), to reveal the extent of SPFH1 and SPFH2 knockdown and exogenous SPFH2 expression (asterisks in lanes 7 and 9) *B*. mHeLa cells were transfected with vectors and exposed to carbachol as in A lanes 1-5 and cell lysates were prepared and probed for IP$_3$R1, SPFH1, SPFH2 and β-actin. Quantitated data are graphed in the lowest panel (n≥4, * denotes p<0.05).
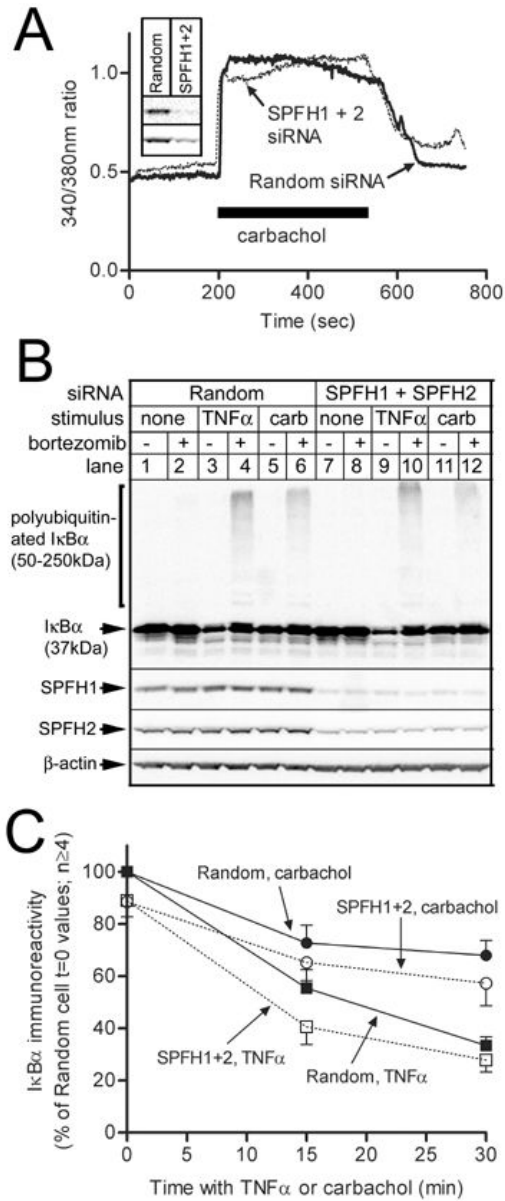
Figure 5. SPFH1 and SPFH2 knockdown does not alter Ca^{2+} signaling or the polyubiquitination of IκBα

mHeLa cells were transfected as in Figure 4 and 72h later were incubated without or with the stimuli indicated. *A*, The 340/380nm ratio (an index of $[Ca^{2+}]$) was measured in individual cells attached to cover slips during perfusion without or with 10μM carbachol (solid bar) and data from four cells for each condition were averaged. The inset shows the levels of SPFH1 (upper panel) and SPFH2 (lower panel) under each condition. *B*, Cells were treated with 2ng/ml TNFα or 1mM carbachol for 30min, without (-) or with (+) a 30min pre-incubation with 1μM bortezomib, and cell lysates were probed for IκBα, SPFH2, SPFH1 and β-actin. The graph shows data from time-courses in which IκBα immunoreactivity at ~37kDa in the absence of bortezomib was quantitated.
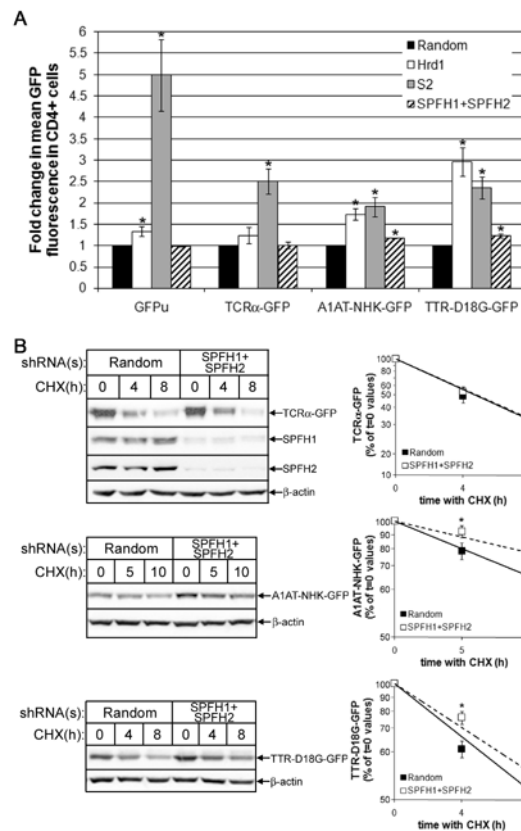
Figure 6. SPFH1 and SPFH2 knockdown stabilizes certain model ERAD substrates
A, HEK cells stably expressing GFPu, TCRα-GFP, A1AT-NHK-GFP or TTR-D18G-GFP
were transfected with vectors encoding Random siRNA or SPFH1si2 plus SPFH2si5 siRNAs
and the GFP fluorescence of CD4+ cells was measured by flow cytometry. Data were
normalized to levels in Random siRNA-expressing cells and graphed as the fold change in
mean GFP fluorescence (n=3, * denotes $p < 0.05$). *B*, HeLa cells were co-transfected with cDNA
encoding TCRα-GFP, A1AT-NHK-GFP or TTR-D18G-GFP together with vectors encoding
Random siRNA or SPFH1si4 plus SPFH2si7 siRNAs, were treated with 20 μg/mL CHX for
the indicated times, and cell lysates were probed for the indicated proteins. Quantitated data
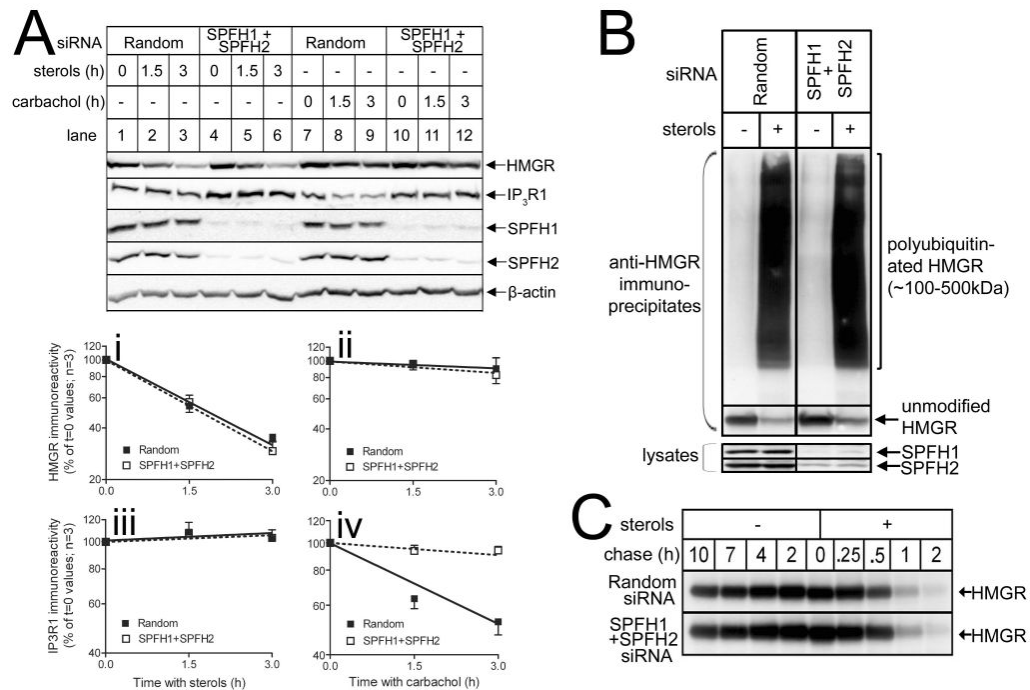are graphed (n≥7, * denotes $p < 0.05$).

Figure 7. SPFH1 and SPFH2 knockdown does not affect the ubiquitination or degradation of HMGR

A. mHeLa cells were transfected with siRNA-encoding vectors as in Figure 4A lanes 1-5, HMGR was up-regulated for 24h, and cells were incubated with either sterols (2μg/ml 25-hydroxycholesterol plus 20μg/ml cholesterol) or carbachol (10μM) as indicated. Cell lysates were then prepared and were probed for HMGR (with A9), IP$_3$R1, SPFH1, SPFH2 and β-actin. Quantitated HMGR and IP$_3$R1 immunoreactivities are shown in graphs i-iv. *B*. Rat1 cells were induced with 1μg/ml doxycycline to express either random or SPFH1/2 siRNAs [23], HMGR was up-regulated for 16h, and cells were treated for 1h with 5μM MG-132 without (-) or with (+) sterols, as indicated. Lysates were then incubated with anti-HMGR membrane region and immunoprecipitates were probed with anti-ubiquitin clone P4D1 or anti-HMGR clone A9. Aliquots of cell lysates were probed with anti-SPFH1 and anti-SPFH2 to assess knockdown (lowest panels). *C*. Rat1 cells were pretreated as in B and were pulse-labeled for 30min with [^{35}S]-methionine/cysteine and chased in the absence or presence of sterols for the indicated times. Lysates were then incubated with anti-HMGR membrane region and radioactivity of immunoprecipitated HMGR was assessed.